Front. Mater. Sci. 2022, 16(2): 220597
https://doi.org/10.1007/s11706-022-0597-5

RESEARCH ARTICLE

In-situ sugar-templated porous elastomer sensor with high sensitivity for wearables

Meng REN[1], Ying FANG[1], Yufan ZHANG[1], Heli DENG[1], Desuo ZHANG[1,2], Hong LIN[1], Yuyue CHEN (✉)[1], and Jiaqing XIONG (✉)[3]

1 College of Textile and Clothing Engineering, Soochow University, Suzhou 215123, China
2 National Engineering Laboratory for Modern Silk, Soochow University, Suzhou 215123, China
3 Innovation Center for Textile Science and Technology, Donghua University, Shanghai 201620, China

ABSTRACT: Fabrication of elastic pressure sensors with low cost, high sensitivity, and mechanical durability is important for wearables, electronic skins and soft robotics. Here, we develop high-sensitivity porous elastomeric sensors for piezoresistive and capacitive pressure detection. Specifically, a porous polydimethylsiloxane (PDMS) sponge embedded with conductive fillers of carbon nanotubes (CNTs) or reduced graphene oxide (rGO) was fabricated by an *in-situ* sugar template strategy. The sensor demonstrates sensitive deformation to applied pressure, exhibiting large and fast response in resistance or capacitance for detection of a wide range of pressure (0–5 kPa). PDMS, as a high-elasticity framework, enables creation of sensors with high sensitivity, excellent stability, and durability for long-term usage. The highest sensitivities of 22.1 and 68.3 kPa^{-1} can be attained by devices with 5% CNTs and 4% rGO, respectively. The geometrics of the sponge sensor is tailorable using tableting technology for different applications. The sensors demonstrate finger motion detection and heart-rate monitoring in real-time, as well as a capacitive sensor array for identification of pressure and shape of placed objects, exhibiting good potential for wearables and human-machine interactions.

KEYWORDS: porous elastomer; sugar template; wearable pressure sensor; graphene; carbon nanotube

Contents

Received January 21, 2022; accepted March 11, 2022

E-mails: chenyy@suda.edu.cn (Y.C.), jqxiong@dhu.edu.cn (J.X.)

1 Introduction

The aging problem of the global population produces demand for more medical equipment and also increases the cost of healthcare. The traditional health monitoring commonly relies on the electrocardiogram, electromyogram, and electroencephalogram to record the bioelectric information from cardiac activity, skeletal muscles, and brain, respectively [1–3]. These bulky analysis instruments rely on the uncomfortable Ag/AgCl gel electrodes and complicated wiring, inconvenient for the aged and for infants that require frequent movement and communication [4]. Wearable sensors show important potential to address or relieve these issues, enabling more economical and reliable solutions to reduce the manpower burden and deliver continuous healthcare monitoring in real-time [5–10].

Flexible pressure sensors are commonly used wearable devices for detecting the external force via transducing their mechanical deformation into electrical signals, and possess advantages of high sensitivity, deformability, and mechanical adaptability. Significant application demands for flexible pressure sensors have emerged in the fields such as wearables [11–14], electronic skins [15–17], soft robotics [18–20], and human-machine interfaces [21–24]. For these interface applications, the lightweight, unobtrusive, and mechanically compliant flexible pressure sensors exhibit enormous potential for human motion detection and healthcare monitoring, such as monitoring of heartbeat, vocal cord vibration, as well as arterial pulsation and sleep status, obtaining important indicators in diagnosis of diseases [25–26]. In terms of working mechanism, pressure sensors are generally divided into three categories, including piezoelectric sensors [27–28], piezoresistive sensors [29–30], and capacitive sensors [31–32]. In comparison with piezoelectric sensors, piezoresistive and capacitive sensors allow more material options such as by use of common polymers and conductive fillers [33].

Important progress has been achieved in combinations of polymer matrixes and conductive nanomaterials, such as nanowires [34], carbon nanotubes [35], carbon nanofibers [36], metal nanoparticles [37] and graphene [38]. These combinations allow production of flexible devices with electrical responses to deformations. Polydimethylsiloxane (PDMS), an intriguing elastomeric matrix, has been widely exploited in wearables. PDMS materials with different geometrics/architectures such as PDMS dense film, microstructural PDMS film, and porous PDMS film have been proved effective as dielectric layers for pressure sensors [39–40]. In comparison, porous elastomer sensors exhibit increased sensitivity due to their high loading ability for functional fillers and superior mechanical responses to external force [41–42]. The porous elastomer devices can be achieved via various manufacturing methods such as breath figures [43], three-dimensional (3D) printing [44] and photolithography technology [45]. But these complex methods are costly and not conducive to wide application. By comparison, the low-cost template methods based on salt [46], sugar [47], organic solvents [48] and polymer microbead stacking [49] have attracted a lot of attention. Long et al. reported a new chemical foaming method using ammonium bicarbonate powder, demonstrating a PDMS-graphene porous material with improved piezoresistive sensing ability [50]. Li et al. prepared porous PDMS based on salt particles through a vacuum-assisted infiltration process, which is a simple processing method that can promote uniformity of pores [51]. The results demonstrated the superiorities of porous elastomer for pressure sensor applications. However, limited efforts have been devoted to developing low-cost fabrication method for reliable porous elastomer pressure sensors.

Efforts have been made to use prepared porous PDMS to adsorb the conductive fillers by dip-coating. However, the adsorbates do not readily infiltrate or adhere stably in the matrix, although they are important for achieving stable performance under the frequent repetition of compressive loading-unloading. To address the above concerns, this article proposes an *in-situ* sugar template strategy to fabricate carbon nanotube (CNT)/PDMS and reduced graphene oxide (rGO)/PDMS sponge pressure sensors. Typically, conductive fillers of CNT or rGO are carried into the PDMS matrix by the granular sugar templates. After tableting and curing, the templates are removed by soaking to generate porous PDMS embedded with CNT or rGO evenly inside the pores. This *in-situ* template strategy based on tableting technology enables controllable geometrics of the sensor by means of changing the pressure, and the conductive fillers can uniformly and tightly attach to the internal surface of PDMS sponges, thus constructing dielectric property or conductive path that are responsive

to external deformations. The sensors with PDMS framework present stable capacitance or resistance responses to the deformations, as well as high sensitivity and mechanical durability. In this work, PDMS sponge sensors are demonstrated to be suitable for detecting finger motion and for heartbeat monitoring, and act as sensor arrays for information mapping of the contact objects. It shows great potential for wearable applications in human motion sensing and healthcare monitoring.

2 Experimental

2.1 Materials

The materials required for the fabrication of CNT/PDMS and rGO/PDMS composite sponges included carbon nanotubes (Jiangsu Xianfeng Nano Material Technology, diameter < 8 nm, length = 0.5–2 μm, purity > 95%), reduced graphene oxide powder (Qingdao Tianyuanda Graphite, thickness = 1–3 nm, layer = 1–5, purity = 98%), sugar cubes (Taikoo), colloidal PDMS polymers and curing agent (Sylgard 184, Dow Corning, USA).

2.2 Fabrication of PDMS sponge sensors

A CNT/PDMS sponge sensor was typically prepared as follows. Sugar cubes were ground into fine particles (<150 μm) for mixing with CNTs, serving as a pores template that carriers with conductive fillers (CNTs). Thereafter, the CNT/sugar particles were completely mixed with PDMS (PDMS:curing agent, 10:1), and the mixture was compressed into a tablet using a tablet machine. The thickness of the tablet could be tuned by controlling the pressure. Thereafter, the tablets were cured in an oven at 80 °C for 12 h, followed by soaking in water for 6 h to fully remove the sugar granules. Owing to the wettability difference, CNTs can be well maintained within the PDMS matrix. Finally, the sample was dried at 60 °C to obtain a porous CNT/PDMS composite material. The content of CNTs in the elastomeric composites was controlled within the range 1%–7% of the mass of PDMS elastomer. Following the same process, rGO was employed to replace the CNTs to fabricate the rGO/PDMS sponges, and 2%–8% rGO was applied to study the sensor performances.

3 Results and discussion

3.1 Fabrication of porous CNT/PDMS and rGO/PDMS elastomer sensors

Figure 1 presents an *in-situ* sugar template strategy for the fabrication of the high-sensitivity and durable pressure sensors based on CNT/PDMS and rGO/PDMS sponges. Typically, conductive fillers of CNT or rGO were mixed with the ground sugar to generate a granular sugar template with conducting components. This granular template was subsequently mixed with PDMS, compressed to tune the sample thickness, thus realizing uniform distribution of the conductive fillers. Followed by curing of the sample at 80 °C for 12 h, the resultant dense elastomer was soaked in water to remove the sugar template. This *in-situ* method enabled the conductive fillers to be well embedded inside the elastomer matrix, thus a porous CNT/PDMS or rGO/PDMS was obtained. As a capacitive or resistive sensor, the device showed excellent sensitivity and high stability, as well as high adaptability to the human body, promising for the wearable pressure sensors.

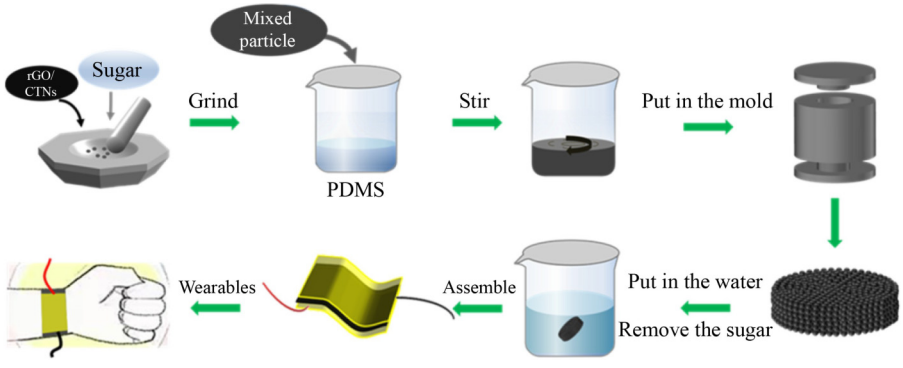

Fig. 1 Schematic fabrication of the porous CNT/PDMS and rGO/PDMS sponges as the wearable sensor.

3.2 Morphology of elastomer sponges

Figure 2 shows photographs and scanning electron microscopy (SEM) images of the elastomer sponges of PDMS, CNT/PDMS, and rGO/PDMS. Firstly, a white appearance was observed on the pure PDMS sponge in Fig. 2(a), suggesting visible light scattering from the uniform porous structure. The cross-section of the sample was observed by SEM, revealing the smooth internal surface of the sponge. In comparison, the CNT/PDMS and rGO/PDMS sponges displayed brown and black appearance, respectively (Figs. 2(b) and 2(c)), indicating that both conductive fillers of CNT and rGO had been evenly incorporated into the porous PDMS matrix. Figure 2(b) presents SEM images of the cross-section to reveal that the CNTs discretely distributed in the pores were embedded in the PDMS matrix. It indicated that the CNTs did not form the continuous conductive path, and only served as conductive fillers to change the dielectric properties of PDMS sponges. This porous elastomer with discrete conductive fillers was thus found to be suitable for the application of capacitive sensor. As revealed by SEM images in Fig. 2(c), the rGO/PDMS sponge showed a very rough internal surface that consisted of a complete combination of PDMS and rGO nanosheets, rendering increased probability of interconnection between the rGO and constructing conductive sponges. It could deliver resistance changes caused by deformation, which is promising for the resistive pressure sensor. Figure 2 verifies that the *in-situ* sugar template strategy could facilitate the physical merger between conductive fillers and the PDMS matrix, which could not only simplify the fabrication process but also enhance the adhesion of the conductive fillers. Good adhesion of the conductive fillers is important to provide stable capacitance or resistance responses for the sponges, ensuring high sensitivity, reliability and durability of the pressure sensors that are subjected to frequent deformation.

3.3 Sensing performance of CNT/PDMS and rGO/PDMS sponges

Since conductive fillers act to tune the dielectric properties or electrical resistance of the elastomer sponges, the optimal ratio of conductive fillers is important for realizing high sensitivity of the devices. By doping CNTs and rGO with different mass fractions, we obtained CNT/PDMS sponges with mass ratios of CNTs ranging from 0% to 7% (CNTs contents of the mass of PDMS), and rGO mass ratios of 2%–7%. Two conductive tapes were attached on both sides of the sponges for sensing performance evaluation. In terms of the assumption from Fig. 2 that CNT fillers were more difficult to form conductive paths compared with rGO filler, CNT/PDMS sponge is more suitable to be designed as capacitive sensor, and rGO/PDMS sponge with more chance to form conductive

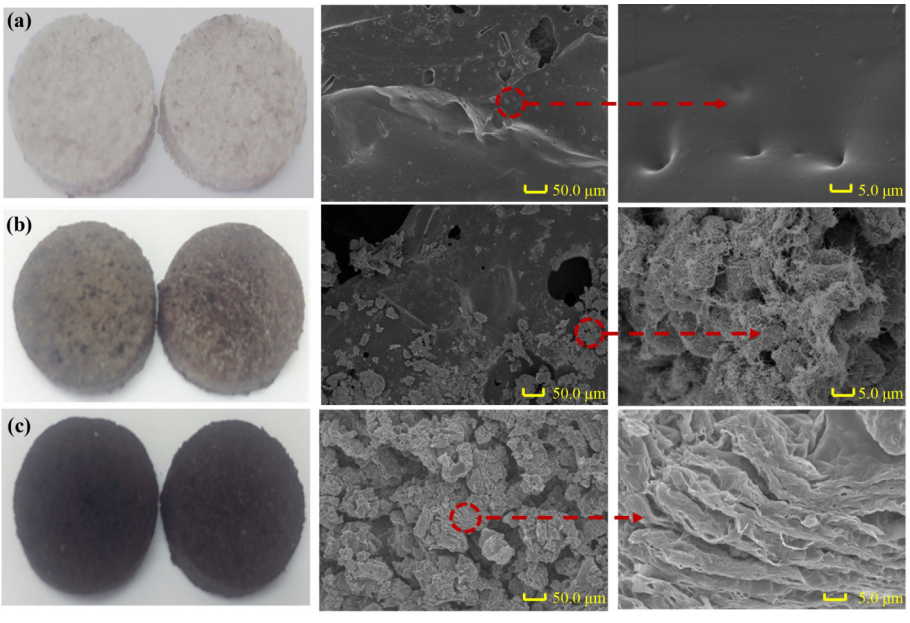

Fig. 2 Photographs and cross-sectional SEM images of the elastomer sponge sensors: (**a**) pure PDMS sponge; (**b**) CNT/PDMS sponge; (**c**) rGO/PDMS sponge.

path is a better candidate for designing as a resistive sensor.

Figure 3(a) shows the capacitance changes of CNT/PDMS sensors with different CNT contents (0%–7%) upon continuously increased pressure of 0–5 kPa. It reveals that all the sensors containing CNTs show higher capacitance responses at the same pressure than those of the pure PDMS sponge sensor, indicating that CNTs could enhance the capacitive sensitivity of the PDMS sponge. The higher capacitance change was achieved at the region of lower pressures, suggesting the sensors exhibited higher sensitivity upon smaller deformations. As the content of CNT increased, the sensitivity of CNT/PDMS sponge first increased and then decreased. The highest sensitivity was achieved at the CNT content of 5%, showing double the increase compared to the control sample without CNTs. It was noticed that there was no positive correlation between the sensitivity and the CNT content. This can be explained by seepage theory that describes the formation of long-range connectivity by nodes or fillers in random systems. When the polymer was mixed with conductive fillers, as the volume fraction of conductive fillers increased, the dielectric constant of the composite material gradually increased, and achieved a maximum value when the volume fraction of conductive fillers reached the percolation threshold. Percolation theory points out that the percolation threshold should have a maximum doping value before the fillers form a continuous conductive path [52]. This phenomenon could therefore be attributed to the ongoing increase of density of the carbon nanotubes as a result of an increased number of electrical junctions between carbon nanotubes, and this finally destroyed the capacitive transmission [53].

Reliability and response time are crucial for pressure sensors. Based on the CNT/PDMS sponge sensor with 5% CNT, the hysteresis of the capacitance change was evaluated by applying and removing the pressure (0–5 kPa). As shown in Fig. 3(b), no obvious hysteresis was observed, suggesting that the sensor can recover in shape and that the CNT fillers can restore their initial locations after release of the pressure. Therefore, a stable capacitance response is attainable and can ensure reliable sensitivity. In addition, the response time of pressure sensors represents their perception ability that mimics the human skin; near-instantaneous response to external stimuli is desired when the sensor is applied for wearables, soft robotics, and human-machine interface, ensuring timely information communication. The capacitance changes of the CNT/PDMS sensor in real-time were monitored to examine its response time under a pressure of 1 kPa. As shown in Fig. 3(c), the sensor had a response time of 0.2 and 0.3 s upon applying the pressure and removing the pressure, respectively, showing good response timeliness among the elastomeric material-based pressure sensors [54–55].

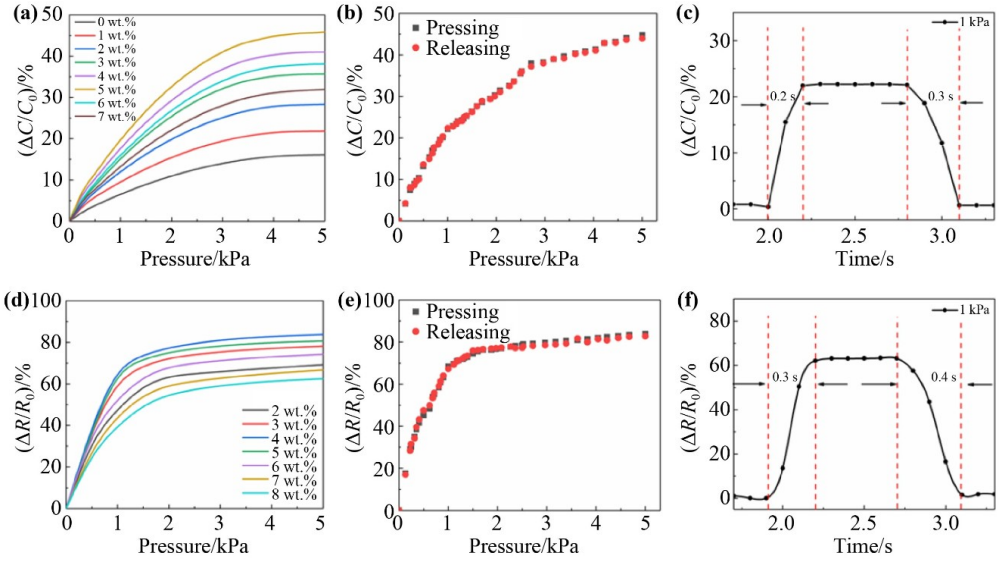

Fig. 3 Sensing performance of CNT/PDMS and rGO/PDMS sponges: (**a**) capacitance change of CNT/PDMS sponges with different doping amounts of CNTs upon pressing; (**b**) capacitance change of a CNT/PDMS sponge (5% CNTs) upon pressing and releasing; (**c**) capacitance response time of a CNT/PDMS sponge (5% CNTs); (**d**) resistance change of rGO/PDMS sponges with different doping amounts of rGO upon pressing; (**e**) resistance change of a rGO/PDMS sponge (4% rGO) upon pressing and releasing; (**f**) resistance response time of a rGO/PDMS sponge (4% rGO).

The rGO/PDMS sponge is more applicable as a resistive sensor. Figure 3(d) shows the resistance change of the rGO/PDMS sponge sensors at different rGO contents (2%–8%) and a pressure range of 0–5 kPa. As the graphene content increased, it displayed a trend that the resistant response increased first and then decreased. The rGO/PDMS sponges exhibited the best sensitivity with a 4% addition of rGO. This was because, with the high content of rGO, the sponge with less PDMS would have much lower elasticity and reduced initial resistance, leading to lower deformations at the same pressure, and also leading to less change in terms of resistance. Besides, the rGO/PDMS showed much higher sensitivity at lower force values, suggesting this sponge with two-dimensional (2D) rGO fillers would easily transform between insulating and conducting states. Therefore, an appropriate ratio between rGO and PDMS matrix is important to maintain the sensor with good elasticity and high sensitivity. Figure 3(e) verifies that the rGO/PDMS sponge sensor with the optimal rGO content of 4% showed negligible hysteresis in resistance change, demonstrating that good recovery ability from deformations was retained. The sensor showed response times of 0.3 and 0.4 s upon 1 kPa pressure application and release, respectively. This was also a compatible response time with the other rGO-based elastomer pressure sensors [56], exhibiting favorable potentials for real-time sensing applications.

3.4 Mechanical durability of PDMS sponge-based sensors

Mechanical durability is another significant property of the flexile pressure sensor, so that stable sensing performance can be maintained and that the device can operate under continuous use and extreme conditions. Based on devices with the optimal sensitivity, cyclic response reliability of CNT/PDMS (5% CNT) and rGO/PDMS (4% rGO) at different compressive strains and working cycles were examined. As shown in Fig. 4(a), the CNT/PDMS capacitive sensor shows an increasing response to the deformation strain from 10% to 30% of the initial thickness of the sponge, but stable capacitance changes were maintained well even after tens of loading-unloading cycles. Furthermore, 200 operation cycles with stable capacitance responses were examined under the 30% compressive strain (Fig. 4(b)). These results verify excellent sensing stability at different deformations, suggesting that the sensor could serve continuously for detection of objects with different weights. The sensor showed good mechanical durability. As shown in Fig. 4(c), two compressive stress–strain curves (0%–30% strain) performed after 300 and 500 cycles coinciding well with each other, which indicated that there is no obvious loss of the elasticity modulus and the sensing reliability of the CNT/PDMS sponge sensor even after 500 cycles of compression.

As shown in Figs. 4(d)–4(f), the same results were

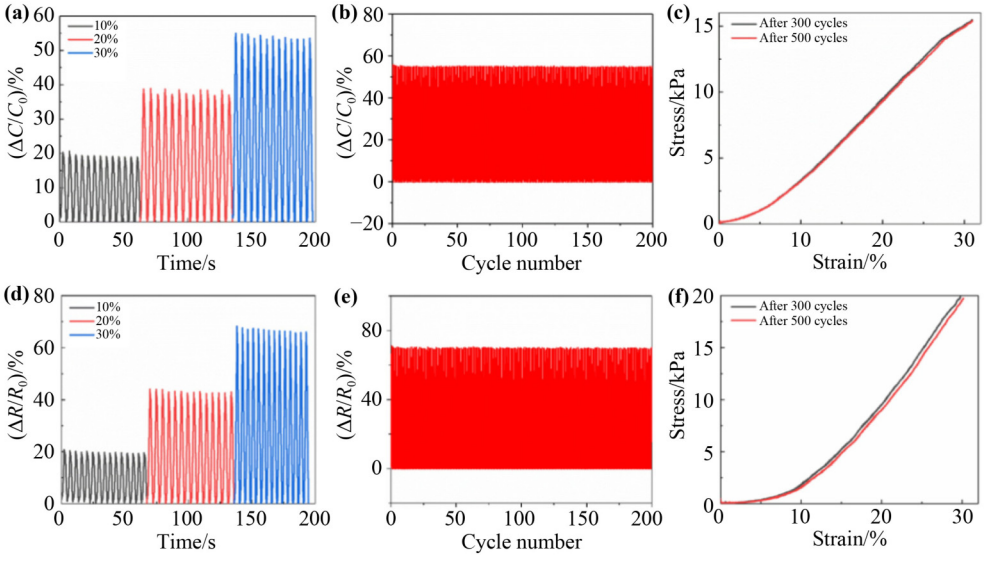

Fig. 4 Cyclic stability of the CNT/PDMS capacitive sensor and the rGO/PDMS resistive sensor: (**a**) capacitance response of CNT/PDMS sponges to compressive deformation; (**b**) compressive durability of the CNT/PDMS capacitive sensor with 30% strain for 200 cycles; (**c**) compressive stress–strain curves of the CNT/PDMS sponge sensor; (**d**) resistance response of rGO/PDMS sponges to compressive deformation; (**e**) compressive durability of the rGO/PDMS resistive sensor with 30% strain for 200 cycles; (**f**) compressive stress–strain curves of the rGO/PDMS sponge sensor.

observed for the resistance response of the rGO/PDMS (4% rGO) sponge sensor. These results confirm advantages of the *in-situ* sugar template strategy in preparing porous PDMS sensors embedded with conductive fillers. The fabrication strategy rendered both high-elasticity porous matrix and tightly adhered conductive fillers that are important in realizing mechanical durability and sensing reliability, which are crucial for long-term usage of the sensors.

3.5 Wearable application of the rGO/PDMS sensor for physiological monitoring

Human motion detection and physiological information monitoring is one of the most important applications of wearable sensors. Herein, the wearable application potential of the rGO/PDMS resistive sensor was evaluated via testing the human physiological information, namely finger bending motion and heart rate. The current response was monitored by applying a fixed voltage to the devices. As shown in Fig. 5(a), the sensor can be fabricated into a sponge sheet and mounted on human finger joints, and it shows rapid resistance response upon bending the finger regardless of immediate release (Fig. 5(b)) or hysteretic release (Fig. 5(c)). This observation indicated that the elastomer sensor can well adapt and detect the deformations induced by finger bending. In addition to these mechanical deformations, the sponge sheet was also investigated as a wrist-based pulse wave detector for heart-rate monitoring (Fig. 5(d)). Figure 5(e) shows the real-time current response to the wrist pulse, and indicates the heart-rate information. It demonstrates that the rGO/PDMS sponge resistive sensor is competent in timely perception of subtle deformations,

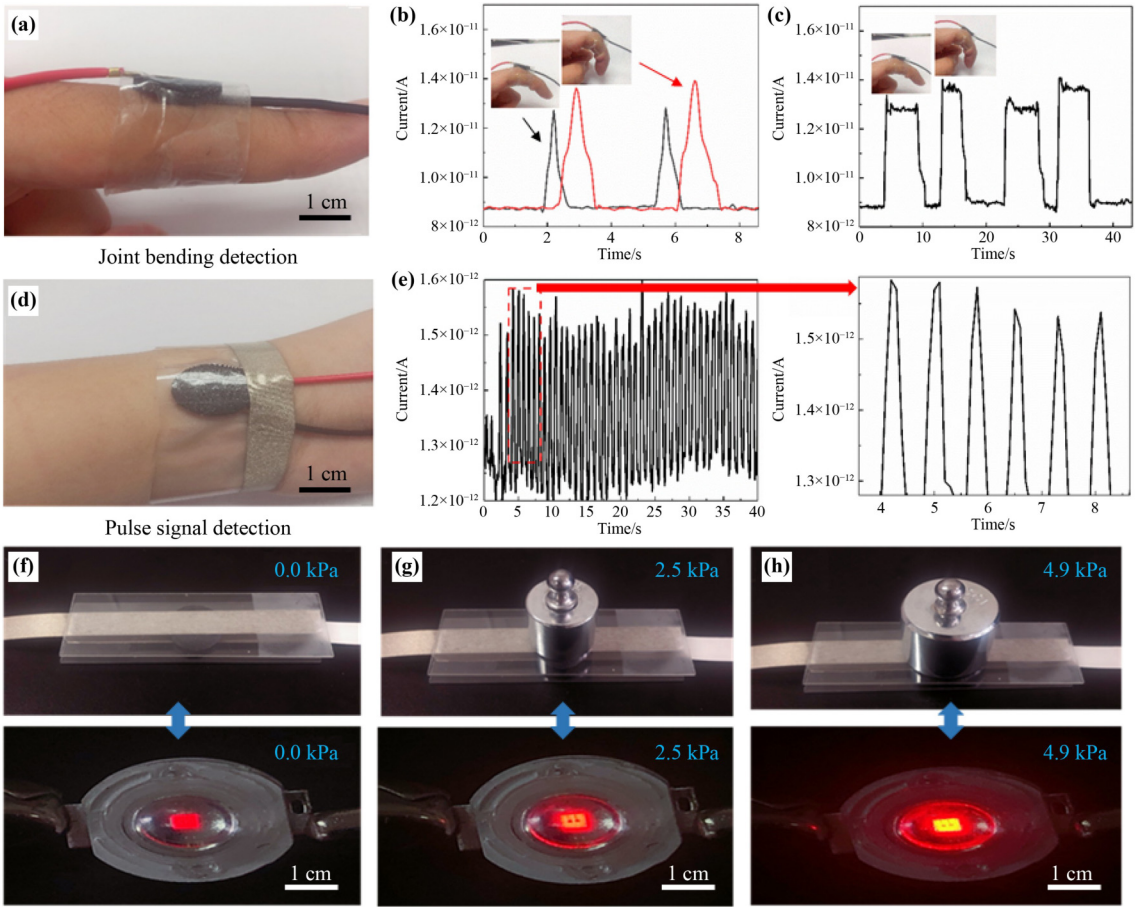

Fig. 5 Wearable applications of the rGO/PDMS resistive sensor: (**a**) a sensor sheet attached to the finger joints; (**b**) current response to straightening of the fingers immediately after bending with different bending angles; (**c**) current response after a finger was bent for a period of time; (**d**) a sensor sheet attached to the wrist; (**e**) heartbeat frequency detection by the sensor; (**f**)(**g**)(**h**) the demonstration of resistance response of the rGO/PDMS sensor upon compression with different forces, in which it served as an electrode for lighting up LEDs (the LED hardly worked when no force was applied on the sensor (panel (f)); the LED started to work when the sensor was subjected to 2.5 kPa pressure (panel (g)); the LED lit well when the sensor was subjected to a pressure of 4.9 kPa (panel (h))).

which is highly meaningful for wearable applications.

In addition, due to the well-embedded rGO in the PDMS matrix, the dynamic electrical connection between the rGO sheets could be realized upon subjecting it to different external forces. A vivid demonstration is presented in Figs. 5(f)–5(h). An rGO/PDMS sponge was employed as an electrode to connect a commercial light-emitting diode (LED); different pressures were applied on the sponge to monitor the brightness of a LED. The LED hardly worked when no pressure was applied to the sponge, indicating that the original rGO/PMDS sponge was nearly insulating (Fig. 5(f)). When the pressure increased from 0 to 4.9 kPa, accordingly, the LED became brighter and brighter (Figs. 5(g) and 5(h)), suggesting that more and more electrical connections were generated when increasing pressure is applied. These results demonstrate the high response of the rGO/PDMS sponge in terms of resistance. The device not only works well as a resistive sensor at the low pressure, but also is capable of serving as an electrode under the high pressures, presenting a multifunctional potential for various application scenarios.

3.6 Application of a sensor array

Another important application the flexible pressure sensor is in serving as electronic skin for soft robotics and human-machine interfaces, identifying pressure distribution or other information during touching operation. Therefore, we designed a capacitive sensor array, allowing a larger sensing area for accurately mapping the pressure due to contacting objects. It was designed based on the principle of parallel plate capacitance, and the sensor unit adopted an array structure formed by cross electrodes, as shown in Fig. 6(a), the gray band-shaped area on the electrode layer is the electrode. It can be assumed that the upper plate has m electrodes and the lower plate has n electrodes. The upper and lower electrodes are vertically distributed in space, forming a total of $m \times n$ capacitor units, so that the capacitance change in each unit can be measured. In order to explore the working efficiency of the sensor, we made a 10×10 flexible array pressure sensor (Fig. 6(b)). The

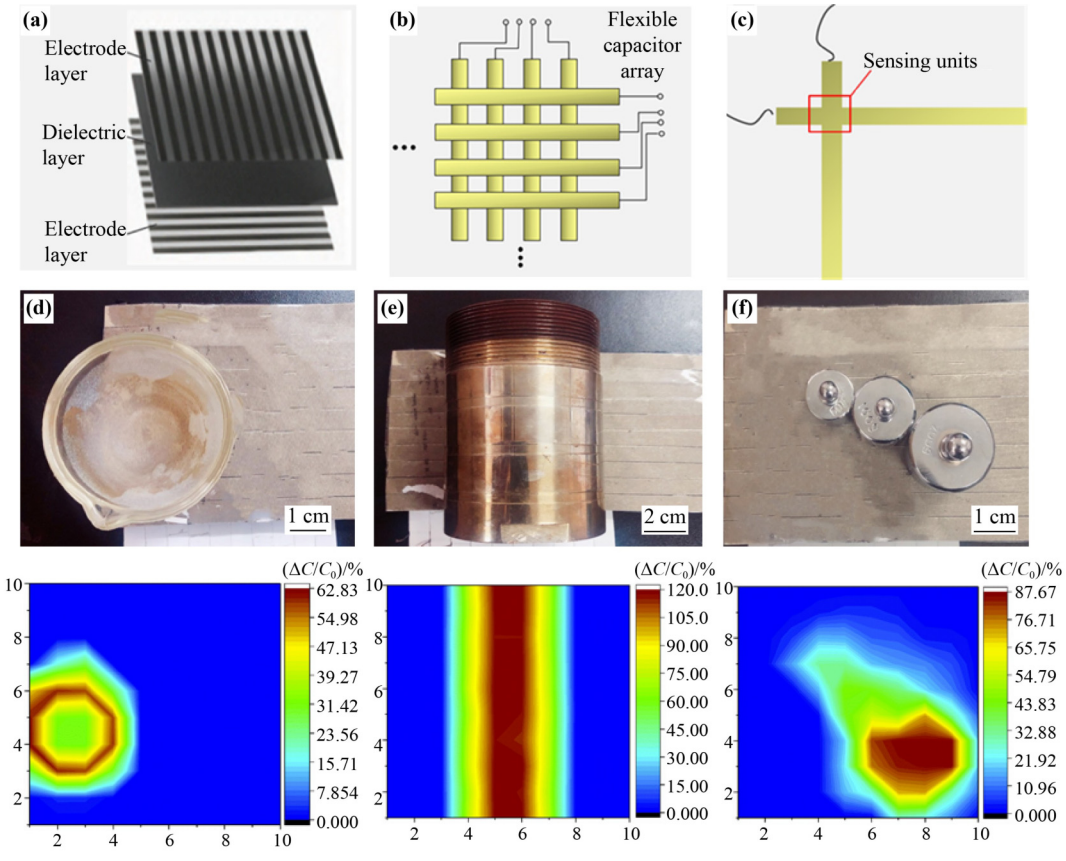

Fig. 6 Capacitance sensor array based on CNT/PDMS sponges: (**a**) schematic configuration of the flexible sensor array; (**b**) flexible capacitive sensor array; (**c**) flexible capacitive sensor unit; (**d**)(**e**)(**f**) capacitance response mappings of the sensor array upon being compressed by a mortar, a reaction kettle and the weights, respectively.

pressure distribution on the sensor surface could be determined by detecting the capacitance of each unit. As shown in Fig. 6(c), the capacitance response of each unit on the sensor could reflect the pressure change in the area. The detection pressure distribution could be realized by collecting the capacitance value of each capacitance unit ($m \times n$) of the sensor. An illustration is presented in Figs. 6(d)–6(f). Different objects including a mortar, a reaction kettle, and three distinct weights were placed on the sensor array, to detect the capacitance change of 100 capacitor units in the sensor. The capacitance value mappings clearly distinguish the different shapes of the objects. Different capacitance changes occurred at corresponding positions on the objects, and greater capacitance change could be observed at the locations that are subjected to the greater weight. It is reasonable to suppose that because the object caused compressive deformation on the sponge dielectric layer, the reduced distance between the upper and lower electrodes led to an increase of the corresponding capacitance. The heavier objects resulted in a smaller distance between electrodes, thus delivering the larger capacitance response. As a lot of capacitive sensor units are required in constructing the array, the repeatable processing, controllable geometrics, and durable elasticity of the CNT/PDMS sponge sensors are crucial for producing a reliable sensor array. The results demonstrated that the capacitive sensor array could not only measure the weight of the placed object but also identify and display the shape and position of the object. It was thus found to be capable of serving as electrical skin for soft-robotics, perceiving the information of external objects.

4 Conclusions

In this study, an *in-situ* expendable template strategy is demonstrated to be effective for the fabrication of porous elastomer-based pressure sensors. Utilizing conductive fillers with different dimensions, such as 1D CNT and 2D rGO, capacitive CNT/PDMS and resistive rGO/PDMS sponge sensors can be realized, with the highest sensitivities of 22.135 and 68.372 kPa^{-1} at contents of 5% CNT and 4% rGO, respectively. Good elasticity of the PDMS sponge framework and favorable adhesion between the conductive fillers and the polymer matrix enables fast response, excellent sensing reliability and mechanical durability of the sensors. The sensors are competent in human motion detection and pulse monitoring, as well as identification of objects, promising as electronic skin for wearables and soft robotics.

Disclosure of potential conflicts of interest The authors declare that they have no conflict of interest.

Acknowledgements This work was supported by the National Natural Science Foundation of China (Grant No. 51403141), the Project Funded by China Postdoctoral Science Foundation (Grant No. 2019M661931), the Prospective Application Research Project on Technology Innovation of Key Industries in Suzhou (Grant No. SYG201936), and the Postgraduate Research & Practice Innovation Program of Jiangsu Province (Grant No. KYCX20_2668).

References

[1] Matsuhisa N, Kaltenbrunner M, Yokota T, et al. Printable elastic conductors with a high conductivity for electronic textile applications. Nature Communications, 2015, 6: 7461

[2] Katsigiannis S, Ramzan N. DREAMER: A database for emotion recognition through EEG and ECG signals from wireless low-cost off-the-shelf devices. IEEE Journal of Biomedical and Health Informatics, 2018, 22(1): 98–107

[3] Geng W, Du Y, Jin W, et al. Gesture recognition by instantaneous surface EMG images. Scientific Reports, 2016, 6(1): 36571

[4] Deignan J, Mcbrearty M, Monedero J, et al. Wearable chemical sensors: characterization of ECG electrodes with electrochemical impedance spectroscopy. Exercise, 2016, 277(5693): 189–192

[5] Xiong J, Chen J, Lee P S. Functional fibers and fabrics for soft robotics, wearables, and human-robot interface. Advanced Materials, 2020, 33(19): 2002640

[6] Kim J, Campbell A S, de Ávila B E, et al. Wearable biosensors for healthcare monitoring. Nature Biotechnology, 2019, 37(4): 389–406

[7] Webb R C, Bonifas A P, Behnaz A, et al. Ultrathin conformal devices for precise and continuous thermal characterization of human skin. Nature Materials, 2013, 12(10): 938–944

[8] Jang K I, Han S Y, Xu S, et al. Rugged and breathable forms of stretchable electronics with adherent composite substrates for transcutaneous monitoring. Nature Communications, 2014, 5(1): 4779

[9] Miyamoto A, Lee S, Cooray N F, et al. Inflammation-free, gas-permeable, lightweight, stretchable on-skin electronics with nanomeshes. Nature Nanotechnology, 2017, 12(9): 907–913

[10] Kim J, Salvatore G A, Araki H, et al. Battery-free, stretchable optoelectronic systems for wireless optical characterization of the skin. Science Advances, 2016, 2(8): e1600418

[11] Xiong J, Cui P, Chen X, et al. Skin-touch-actuated textile-based triboelectric nanogenerator with black phosphorus for durable biomechanical energy harvesting. Nature Communications, 2018, 9(1): 4280

[12] Xiong J, Lin M F, Wang J, et al. Wearable all-fabric-based triboelectric generator for water energy harvesting. Advanced Energy Materials, 2017, 7(21): 1701243

[13] Hua Q, Sun J, Liu H, et al. Skin-inspired highly stretchable and conformable matrix networks for multifunctional sensing. Nature Communications, 2018, 9(1): 244

[14] Kim J, Kim M, Lee M S, et al. Wearable smart sensor systems integrated on soft contact lenses for wireless ocular diagnostics. Nature Communications, 2017, 8(1): 14997

[15] Lu N, Kim D H. Flexible and stretchable electronics paving the way for soft robotics. Soft Robotics, 2014, 1(1): 53–62

[16] Schwartz G, Tee B C K, Mei J, et al. Flexible polymer transistors with high pressure sensitivity for application in electronic skin and health monitoring. Nature Communications, 2013, 4(1): 1859

[17] Wang C, Hwang D, Yu Z, et al. User-interactive electronic skin for instantaneous pressure visualization. Nature Materials, 2013, 12(10): 899–904

[18] Wang C, Xia K, Zhang M, et al. An all-silk-derived dual-mode e-skin for simultaneous temperature–pressure detection. ACS Applied Materials & Interfaces, 2017, 9(45): 39484–39492

[19] Wang Q, Jian M, Wang C, et al. Carbonized silk nanofiber membrane for transparent and sensitive electronic skin. Advanced Functional Materials, 2017, 27(9): 1605657

[20] Gao D, Wang J, Ai K, et al. Inkjet-printed iontronics for transparent, elastic, and strain-insensitive touch sensing matrix. Advanced Intelligent Systems, 2020, 2(7): 2000088

[21] Honda W, Harada S, Arie T, et al. Wearable, human-interactive, health-monitoring, wireless devices fabricated by macroscale printing techniques. Advanced Functional Materials, 2014, 24(22): 3299–3304

[22] Tao L Q, Tian H, Liu Y, et al. An intelligent artificial throat with sound-sensing ability based on laser induced graphene. Nature Communications, 2017, 8(1): 14579

[23] Li Y, Samad Y A, Liao K. From cotton to wearable pressure sensor. Journal of Materials Chemistry A: Materials for Energy and Sustainability, 2015, 3(5): 2181–2187

[24] Shi X, Zuo Y, Zhai P, et al. Large-area display textiles integrated with functional systems. Nature, 2021, 591(7849): 240–245

[25] Chen X, Parida K, Wang J, et al. A stretchable and transparent nanocomposite nanogenerator for self-powered physiological monitoring. ACS Applied Materials & Interfaces, 2017, 9(48): 42200–42209

[26] Fan W, He Q, Meng K, et al. Machine-knitted washable sensor array textile for precise epidermal physiological signal monitoring. Science Advances, 2020, 6(11): eaay2840

[27] Wu F, Chen S, Chen B, et al. Bioinspired universal flexible elastomer-based microchannels. Small, 2018, 14(18): 1702170

[28] Dagdeviren C, Su Y, Joe P, et al. Conformable amplified lead zirconate titanate sensors with enhanced piezoelectric response for cutaneous pressure monitoring. Nature Communications, 2014, 5(1): 4496

[29] Yan C, Wang J, Kang W, et al. Highly stretchable piezoresistive graphene-nanocellulose nanopaper for strain sensors. Advanced Materials, 2014, 26(13): 2022–2027

[30] Liu H, Dong M Y, Huang W J, et al. Lightweight conductive graphene/thermoplastic polyurethane foams with ultrahigh compressibility for piezoresistive sensing. Journal of Materials Chemistry C: Materials for Optical and Electronic Devices, 2017, 5(1): 73–83

[31] Cho S H, Lee S W, Yu S, et al. Micropatterned pyramidal ionic gels for sensing broad-range pressures with high sensitivity. ACS Applied Materials & Interfaces, 2017, 9(11): 10128–10135

[32] Mannsfeld S C B, Tee B C K, Stoltenberg R M, et al. Highly sensitive flexible pressure sensors with microstructured rubber dielectric layers. Nature Materials, 2010, 9(10): 859–864

[33] Li J, Fang L, Sun B, et al. Recent progress in flexible and stretchable piezoresistive sensors and their applications. Journal of the Electrochemical Society, 2020, 167(3): 037561

[34] Gong S, Lai D T H, Su B, et al. Highly stretchy black gold e-skin nanopatches as highly sensitive wearable biomedical sensors. Advanced Electronic Materials, 2015, 1(4): 1400063

[35] Shi J, Li X, Cheng H, et al. Graphene reinforced carbon nanotube networks for wearable strain sensors. Advanced Functional Materials, 2016, 26(13): 2078–2084

[36] Jian M, Wang C, Wang Q, et al. Advanced carbon materials for flexible and wearable sensors. Science China Materials, 2017, 60(11): 1026–1062

[37] Lee J, Kim S, Lee J, et al. A stretchable strain sensor based on a metal nanoparticle thin film for human motion detection. Nanoscale, 2014, 6(20): 11932–11939

[38] Boland C S, Khan U, Ryan G, et al. Sensitive electromechanical sensors using viscoelastic graphene–polymer nanocomposites. Science, 2016, 354(6317): 1257–1260

[39] Tee B C K, Chortos A, Dunn R R, et al. Tunable flexible pressure sensors using microstructured elastomer geometries for intuitive electronics. Advanced Functional Materials, 2014, 24(34): 5427–5434

[40] Wang H, Xiang Z, Giorgia P, et al. Triboelectric liquid volume sensor for self-powered lab-on-chip applications. Nano Energy, 2016, 23: 80–88

[41] Xiong J, Thangavel G, Wang J, et al. Self-healable sticky porous

elastomer for gas–solid interacted power generation. Science Advances, 2020, 6(29): eabb4246

[42] Sun B, McCay R N, Goswami S, et al. Gas-permeable, multifuncationl on-skin electronics based on laser-induced porous graphene and sugar-templated ealstomer sponges. Advanced Materials, 2018, 30(50): 1804327

[43] Miller S, Bao Z. Fabrication of flexible pressure sensors with microstructured polydimethylsiloxane dielectrics using the breath figures method. Journal of Materials Research, 2015, 30(23): 3584–3594

[44] Deng Z, Hu T, Lei Q, et al. Stimuli-responsive conductive nanocomposite hydrogels with high stretchability, self-healing, adhesiveness, and 3D printability for human motion sensing. ACS Applied Materials & Interfaces, 2019, 11(7): 6796–6808

[45] Zhang L, Liu L, Liu C, et al. Photolithographic fabrication of graphene-based all-solid-state planar on-chip microsupercapacitors with ultrahigh power characteristics. Journal of Applied Physics, 2019, 126(16): 164308

[46] Tyagi P, Chaturvedi R, Gorhe N R. Macroporous poly(vinyl chloride)-polypyrrole composites with piezoresistive behaviour. Materials Letters, 2020, 280: 128566

[47] Wu S, Zhang J, Ladani R B, et al. Novel electrically conductive porous PDMS/carbon nanofiber composites for deformable strain sensors and conductors. ACS Applied Materials & Interfaces, 2017, 9(16): 14207–14215

[48] Kim Y, Jang S, Oh J H. Fabrication of highly sensitive capacitive pressure sensors with porous PDMS dielectric layer via microwave treatment. Microelectronic Engineering, 2019, 215: 111002

[49] Kang S, Lee J, Lee S, et al. Highly sensitive pressure sensor based on bioinspired porous structure for real-time tactile sensing. Advanced Electronic Materials, 2016, 2(12): 1600356

[50] Long Y, Zhao X, Jiang X, et al. A porous graphene/polydimethylsiloxane composite by chemical foaming for simultaneous tensile and compressive strain sensing. FlatChem, 2018, 10: 1–7

[51] Li Q, Duan T, Shao J, et al. Fabrication method for structured porous polydimethylsiloxane (PDMS). Journal of Materials Science, 2018, 53(16): 11873–11882

[52] Mamunya Y P, Muzychenko Y V, Pissis P, et al. Percolation phenomena in polymers containing dispersed iron. Polymer Engineering and Science, 2002, 42(1): 90–100

[53] Kou H, Zhang L, Tan Q, et al. Wireless flexible pressure sensor based on micro-patterned graphene/PDMS composite. Sensors and Actuators A: Physical, 2018, 277: 150–156

[54] Al-Handarish Y, Omisore O M, Duan W, et al. Facile fabrication of 3D porous sponges coated with synergistic carbon black/multiwalled carbon nanotubes for tactile sensing applications. Nanomaterials, 2020, 10(10): 1941

[55] Park S W, Das P S, Park J Y. Development of wearable and flexible insole type capacitive pressure sensor for continuous gait signal analysis. Organic Electronics, 2018, 53: 213–220

[56] Tang X, Wu C, Gan L, et al. Multilevel microstructured flexible pressure sensors with ultrahigh sensitivity and ultrawide pressure range for versatile electronic skins. Small, 2019, 15(10): 1804559